Pramana – J. Phys. (2017) 88: 28
DOI 10.1007/s12043-016-1337-0

Solitons, compactons and undular bores in Benjamin–Bona–Mahony-like systems

APARNA SAHA[1], B TALUKDAR[1,*], UMAPADA DAS[2] and SUPRIYA CHATTERJEE[3]

[1]Department of Physics, Visva Bharati University, Santiniketan 731 235, India
[2]Department of Physics, Abhedananda College, Sainthia 731 234, India
[3]Department of Physics, Bidhannagar College, EB-2, Sector-1, Salt Lake, Kolkata 700 064, India
*Corresponding author. E-mail: binoy123@bsnl.in

MS received 22 January 2016; revised 25 June 2016; accepted 20 July 2016; published online 4 January 2017

Abstract. We examine the effect of dissipation on travelling waves in nonlinear dispersive systems modelled by Benjamin–Bona–Mahony (BBM)-like equations. In the absence of dissipation, the BBM-like equations are found to support soliton and compacton/anticompacton solutions depending on whether the dispersive term is linear or nonlinear. We study the influence of increasing nonlinearity of the medium on the soliton and compacton dynamics. The dissipative effect is found to convert the solitons either to undular bores or to shock-like waves depending on the degree of nonlinearity of the equations. The anticompacton solutions are also transformed to undular bores by the effect of dissipation. But the compactons tend to vanish due to viscous effects. The local oscillatory structures behind the bores and/or shock-like waves in the case of solitons and anticompactons are found to depend sensitively both on the coefficient of viscosity and solution of the unperturbed problem.

Keywords. Benjamin–Bona–Mahony-like equations; travelling wave solutions; solitons; compactons; dissipation; undular bores; shock waves.

PACS Nos 02.30.Gp; 02.30.Hq; 02.30.Jr

1. Introduction

It is fairly well known that Korteweg–de Vries (KdV) equation

$$u_t + u_x + uu_x + u_{xxx} = 0, \quad u = u(x,t), \tag{1}$$

which could model the generation of solitons on the surface of water, possesses many remarkable properties. For example, the investigation of conservation laws of the equation led to the discovery of a wide variety of ingenuous mathematical techniques including the Muira transformation, Lax-pair representation, inverse scattering method and bi-Hamiltonian structure that were subsequently used to examine the integrability of other similar equations. But it is less well known that (1) has an unbounded dispersion relation. This awkward physical constraint can be realized in terms of the linearized form $u_t + u_x + u_{xxx} = 0$ of the KdV equation. Assuming the solution of the linear equation as a summation of Fourier component $f(k)\mathrm{e}^{-i(kx-wt)}$ we obtain the dispersion relation $\omega(k) = k - k^3$. The corresponding phase velocity v_p $(=\omega(k)/k) = 1 - k^2$ becomes negative for $k^2 > 1$. This contradicts our initial assumption for the forward travelling wave. Moreover, the group velocity v_g $(=\mathrm{d}\omega/\mathrm{d}k) = 1 - 3k^2$ has no lower bound.

To circumvent the above difficulties, originally Peregrine [1] and subsequently Benjamin, Bona and Mahony [2] proposed the equation

$$u_t + u_x + uu_x - u_{xxt} = 0 \tag{2}$$

as an alternative model for the motion of long waves in nonlinear dispersive systems. The linearized version of (2) leads to the dispersion relation $\omega(k) = k/(1 + k^2)$ such that both v_p and v_g are well behaved for all values of k. Thus, as opposed to the KdV equation, (2) provides us with a regularized long-wave (RLW) equation. Benjamin *et al* [2] established that both (1) and (2) are valid at the same level of approximation but in applicative context the latter equation does have some advantages over the KdV equation. As a result, (2) is often called the Benjamin–Bona–Mahony or BBM equation.

In order to understand the role of nonlinear dispersion in the formation of patterns in waves governed by the RLW model, Yandong [3] and Wang *et al* [4] considered a family of BBM-like equations

$$u_t + u_x + a(u^m)_x - (u^n)_{xxt} = 0, \quad m \geq 2, \quad n \geq 1. \quad (3)$$

For $m = 2$, $a = 1/m$ and $n = 1$, (3) reduces to the usual BBM equation. The equation is more nonlinear than the usual BBM equation for $m > 2$. For $n > 1$ the dispersive term in (3) is nonlinear. Evolution equations with nonlinear dispersive terms were first considered by Rosenau and Hyman [5]. In particular, the equation

$$u_t + (u^m)_x + (u^n)_{xxx} = 0, \quad m > 1, \quad 1 < n \leq 3 \quad (4)$$

was used by them as a model that could account for the formation of patterns in liquids. It was demonstrated that the travelling wave solutions of (4) are free from the usual exponential tails of solitons and vanish identically outside a finite range. These solutions were given the name compactons. The compactons are robust within their range of existence. However, unlike the interaction of solitons in the KdV-like systems, the point at which two compactons collide is marked by the birth of a low-amplitude compacton–anticompacton pair.

A straightforward generalization to the family of equations given in (3) to include the effect of viscosity is provided by

$$u_t + u_x + a(u^m)_x - (u^n)_{xxt} = \eta u_{xx}, \quad (5)$$

where η is the kinematic viscosity coefficient. Recently, Mancas *et al* [6] derived a formalism to write the general solution of (5) for $n = 1, m = 2$ and $a = 1/m$, and demonstrated that in the case of BBM equations there still exist, in certain region of space, bounded travelling wave solutions in the form of solitons. The results of these authors appear to substantiate a general remark made by El *et al* [7] who claimed that introduction of small dissipation in a nonlinear system dramatically changes its properties, allowing in some cases for the presence of steady solution.

In this paper, we shall first construct analytical solutions of (3) for $n = 1$ and 2, and in each case we shall consider different values of m with a view to illustrate how the solutions behave as the systems become more and more nonlinear. We then turn our attention to study the effect of dissipation on the system modelled by (3). We shall achieve this by solving (5) and comparing its solutions with the appropriate solutions of (3). It appears that the mathematical approach developed in ref. [6] which was used to solve the initial boundary value problem for the dissipative BBM equation ($m = 2$ and $n = 1$) is not applicable to (5). In view of this, we convert the equation to a Cauchy problem in an appropriate coordinate system and solve it by using numerical methods. Interestingly, we find that solutions of the dissipative system, in general, do not represent bounded travelling waves. On the other hand, the solution obtained by us for any chosen set of values for n, m and η resembles either the so-called undular bores or shock waves. As with shock-like waves, the bore is a well-known phenomenon in fluid mechanics, describing the transition between two uniform streams with different flow depths [8]. Undular bores feature free surface oscillations behind the front of the bore, and one says that the bore is purely undular if none of the waves behind the bore is breaking [9].

In this context, we note that there has been a resurgence of interest in studying the formation of patterns in waves governed by Rosenau–Hyman-like and RLW equations by using either the methods of dynamical systems theory [10] or some special techniques for solving nonlinear evolution equations [11,12]. It has been recognized that often shock waves and singular soliton solutions cannot be found by the travelling-wave approach. This disadvantage of working with the travelling-wave hypothesis can, however, be remedied by taking recourse to the use of a different method of integrability known as the ansatz method [13]. Recently, Sanchez [14] made use of this method in conjunction with the so-called soliton perturbation theory to obtain families of exact solutions of the improved Korteweg–de Vries equation with power-law nonlinearity.

In §2 we introduce the so-called travelling coordinates and use it to convert the partial differential equation in (3) to a nonlinear ordinary differential equation and subsequently write the latter as a dynamical system. We provide necessary phase-plane analysis to study the behaviour of the nonlinear system. We also present plots of the vector fields with which we can model the speed and direction of a moving fluid throughout the space. All results are presented with a view to examine the effects of varying nonlinearity and dispersion (different values of m and n) on the soliton and compacton solutions in the non-dissipative medium. In §3 we examine the effects of dissipation on the wave motion in BBM-like systems. As opposed to the case studies presented in §2, here we take recourse to the use of numerical routines to deal with eq. (5). We find that due to viscous effects the solitons and compactons are converted either to undular bores or shock-like waves, the exact nature of which depends

on the values of m and n. Finally in §4 we summarize our outlook on the present problem and make some concluding remarks.

2. Nondissipative BBM-like systems

Equation (3) which models a family of nondissipative BBM-like systems for different values of m and n does not involve the space and time coordinates explicitly. Consequently, the equation is invariant under translation in these variables and can, therefore, be reduced to a nonlinear ordinary differential equation using the travelling coordinate $\xi = x - vt$ where v is the nonzero translational wave velocity. Keeping this in mind we apply the change of variable

$$u(x,t) = \phi(x - vt) \tag{6}$$

in (3) and obtain the ordinary differential equation

$$(1-v)\phi' + a(\phi^m)' + v(\phi^n)''' = 0, \tag{7}$$

where primes denote differentiation with respect to ξ. Integration of (7) with respect to ξ yields

$$(1-v)\phi + a(\phi^m) + v(\phi^n)'' = 0. \tag{8}$$

In writing (8), as in ref. [2], we have taken the constant of integration equal to zero. This choice will allow us to reproduce, in the appropriate limit, all results of the BBM equation from the solutions of (8). We now make a further change in the dependent variable of (8) by writing $\phi = y^{1/n}$ and express the transformed equation in the form

$$y'' + \frac{a}{v}y^{m/n} + \frac{1-v}{v}y^{1/n} = 0. \tag{9}$$

To treat (9) by the methods of dynamical systems theory [15] we rewrite the equation as a system of first-order differential equations

$$z = y', \quad z = z(\xi) \tag{10a}$$

and

$$z' = -\frac{a}{v}y^{m/n} - \frac{1-v}{v}y^{1/n}. \tag{10b}$$

On the other hand, we could multiply (9) by y' and integrate once to get

$$c = \frac{n(1-v)}{n+1}y^{(n+1)/n} + \frac{an}{m+n}y^{(m+n)/n} + \frac{v}{2}y'^2, \tag{11}$$

where c is a constant of integration. Since (9) is an autonomous differential equation without explicit time dependence, the constant c can be identified with the Hamiltonian of the system. The set of equations as given in (10) can be used to draw the phase portrait while (11) can be used to plot the vector fields. The first-order equation (11) can easily be integrated to write y as a function of ξ for all values of c. This gives solution of the BBM-like equation for given values of m and n.

In terms of ϕ, (10a) and (10b) read as

$$z = n\phi^{n-1}\psi, \quad \psi = \phi' \tag{12a}$$

and

$$z' = -\frac{a}{v}\phi^m - \frac{1-v}{v}\phi. \tag{12b}$$

It is straightforward to combine (12a) and (12b) to write

$$z = \pm\sqrt{\frac{2n\phi^n}{v}\left(\frac{v-1}{n+1}\phi - \frac{a}{m+n}\phi^m\right)}. \tag{13}$$

Equations (12) and (13) can now be used to plot the phase trajectories on the (ϕ, ψ) plane. In terms of ϕ and ψ, the constant c in (11) can be written as

$$c = \frac{n}{n+1}(1-v)\phi^{n+1} + \frac{an}{m+n}\phi^{m+n} + \frac{vn^2}{2}\phi^{2(n-1)}\psi^2. \tag{14}$$

In the following we use eq. (14) to present the phase portrait, vector plot and travelling wave solution of (3) for specific values of n and m. We divide our computed results into two distinct classes depending on the values of n (1 or 2). Independently of the values of m, the dispersive term in each equation for $n = 1$ is linear while such a dispersive term is nonlinear for any equation with $n = 2$. We shall present all numerical results for $v = 1.5$.

2.1 *Equations with linear dispersive term* ($n = 1$)

Here we begin with $m = 2$ and then consider equations for higher values of m. We shall see that, for all values of m, the equations support soliton solutions although their phase trajectories and vector fields are quite different. As m increases we, however, observe regularity for changes in the phase-space structure and associated vector field.

(a) $m = 2$: In this case, (3) gives the BBM equation. The associated phase portrait and vector field are given in figures 1 and 2. We calculated the phase trajectory using (12) and (13). The vector field was generated from the integral curve in (14).

A phase path that separates obvious distinct regions in the phase plane is known as the separatrix. The phase path in figure 1 joins the saddle-type equilibrium (0, 0) to itself by enclosing a centre-type equilibrium point at (1, 0) and is thus a form of separatrix often known as the homoclinic path. From figure 2 we see that at all points the vector field diverges from the critical point (0, 0) while similar tangent vectors converge towards (1, 0). This reconfirms that the equilibrium point (0, 0) is a saddle and (1, 0) is a centre. For $c = 0$, $n = 1$, $m = 2$ and $v = 1.5$, from (14) we obtain the soliton solution of the BBM equation as

$$\phi(\xi) = 1.5\,\mathrm{sech}^2(0.288675\xi). \tag{15}$$

Clearly, the soliton has an amplitude 1.5 and moves to the right with speed 1.5 m/s. Initially, it is centred at the point $x = 0$.

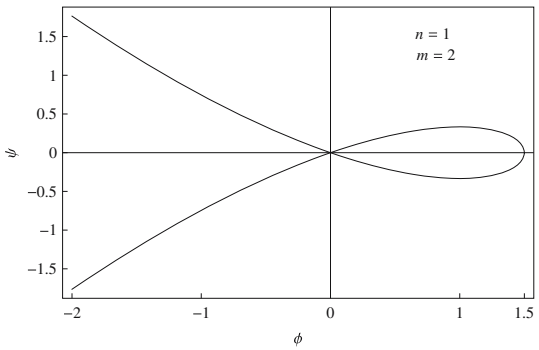

Figure 1. Phase diagram of the BBM equation, eq. (3), when $n = 1$, $m = 2$.

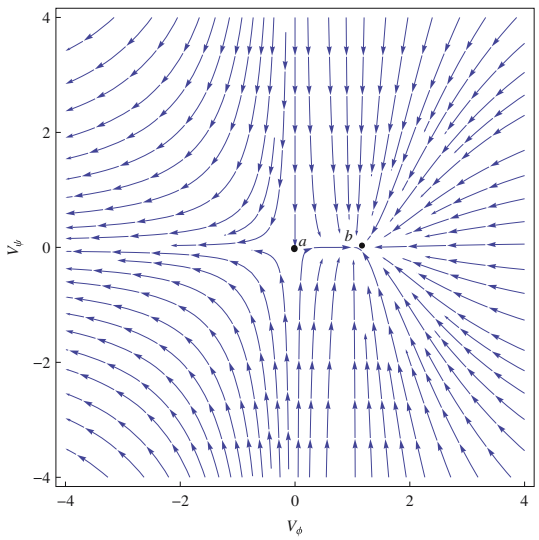

Figure 2. Vector flow for the integral curve (14) for BBM equation. The coordinates $V_\phi = -\partial c/\partial\phi$ and $V_\psi = -\partial c/\partial\psi$. The orientation of the line segment indicates the slope $\mathrm{d}\psi/\mathrm{d}\phi$ at the centre of the segment.

(b) $m = 3$: In this case, (3) leads to an equation which is more nonlinear than the BBM equation. The present nonlinear equation appears to be the RLW analog of the modified KdV equation. We display in figure 3 the appropriate phase diagram. Here the phase trajectory is a closed homoclinic path that joins the saddle-type equilibrium point (0, 0) to itself but, as opposed to the curve in figure 1, the phase path now encircles the equilibrium points (±1.22474, 0). The solution of the BBM-like equation for $m = 3$ is given by

$$u(x, t) = 1.73\,\mathrm{sech}(0.577350\,\xi). \tag{16}$$

From (15) and (16) we see that the soliton solution for $m = 3$ depends linearly on the sech function while that for $m = 2$ with quadratic dependence on sech function closely resembles the KdV soliton. Moreover, the argument of the sech function in (16) is exactly twice the argument of the sech function that appears in (15). The soliton in (16) is taller than that in (15).

(c) $m = 4$: In this case, the equation is still more nonlinear. The associated phase diagram is shown in figure 4. The phase path in figure 4 is similar to that in figure 1 with a saddle point (0, 0) and centre

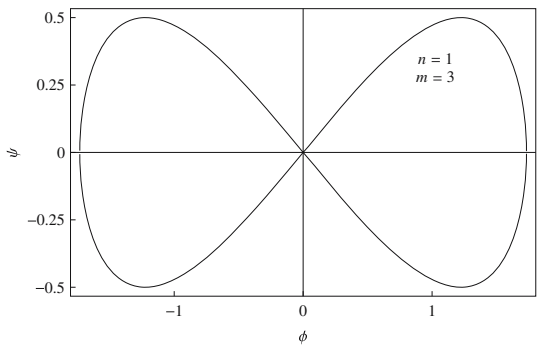

Figure 3. Phase diagram of eq. (3), when $n = 1$, $m = 3$.

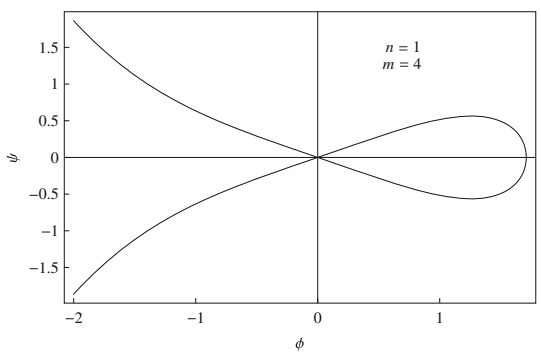

Figure 4. Phase diagram of eq. (3), when $n = 1$, $m = 4$.

(1.25994, 0). As expected, the vector field diverges from (0, 0) and converges towards (1.25994, 0). The solution of (3) for $m = 4$ is found to be

$$u(x,t) = 1.71\,\mathrm{sech}^{2/3}(0.866025\xi). \tag{17}$$

Note that $u(x,t)$ now has $\mathrm{sech}^{2/3}$ dependence. The height of the soliton in (17) is greater than that of the soliton in (15) but less than the height of the soliton in (16).

The phase diagram and vector field of (3) for $m = 4$ are identical to those of the same equation for $m = 2$. We found similar agreement between the results of equations for $m = 5$ and $m = 3$. In fact, by considering the phase diagrams and vector plots for still higher values of m, we arrived at a conclusion that, so far as the dynamical behaviour is concerned, the BBM-like equations in (3) with linear dispersive term can be divided into two distinct classes depending on whether m is even or odd. All equations with even values of m are characterized by two equilibrium points of which one is a saddle and the other is a centre. But equations with odd values of m possess three equilibrium points – one is of saddle type and two others are centres.

The centre-type equilibrium point is a sink or attracting fixed point. The saddle-type equilibrium point is a source or repelling fixed point. Thus, from the above we infer that equations with even m values physically refer to fluid motion characterized by one source and one sink. On the other hand, equations with odd m values describe motion of fluids in which there are one source point and two sinks.

The solution of (3) for $n = 1$ and an arbitrary value of m can be written in the form

$$u(x,t) = \left[\frac{m(m+1)(v-1)}{2}\right]^{1/(m-1)} \times \mathrm{sech}\left[\frac{1}{2}(m-1)\sqrt{\frac{v-1}{v}}\xi\right]^{2/(m-1)}. \tag{18}$$

We use the general expression (18) to compute $u(x,t)$ as a function of ξ for $m > 4$. From these results we found that the width of the soliton continuously decreases as m increases. But the amplitude of the soliton first increases from 1.5 to 1.73 as m goes from 2 to 3, then the amplitude decreases and tends to 1 as m increases.

2.2 *Equations with nonlinear dispersive term* ($n = 2$)

For $n \geq 2$, the dispersive terms of all equations obtained from (3) are nonlinear. For illustrative purposes we shall consider the case $n = 2$ only and vary the values of m in order to study the effect of higher nonlinearities on the compacton solution supported by the BBM-like equations with nonlinear dispersive terms.

(a) $m = 2$: Here the equation obtained from (8) is given by

$$\phi'' = \frac{v-1}{2v} - \frac{\phi}{4v} - \frac{\phi'^2}{\phi}. \tag{19}$$

By writing (18) as two first-order differential equations

$$\psi = \phi' \tag{20a}$$

and

$$\psi' = \frac{v-1}{2v} - \frac{\phi}{4v} - \frac{\phi'^2}{\phi} \tag{20b}$$

we find that (19) has only one equilibrium point $E_1(2(v-1), 0)$. Linear stability analysis [15] can now be used to show that $E_1(2(v-1), 0)$ is a centre-type equilibrium point. Note that for the linear dispersive equation corresponding to that in (19) had two equilibrium points – one centre and other saddle (figure 1). We display the phase diagram for (19) in figure 5. The phase trajectory shown for $v = 1.5$ is a closed orbit about the equilibrium point and does not approach $E_1(1, 0)$ as $t \to \pm\infty$. The perturbation of the system neither decays to zero nor diverges to infinity but it varies periodically with time. As a result, such centre-type equilibrium points are often referred to as neutrally stable. Since the centre always serves as a sink, the vector field in this case is always directed towards the equilibrium point of (19). We shall not

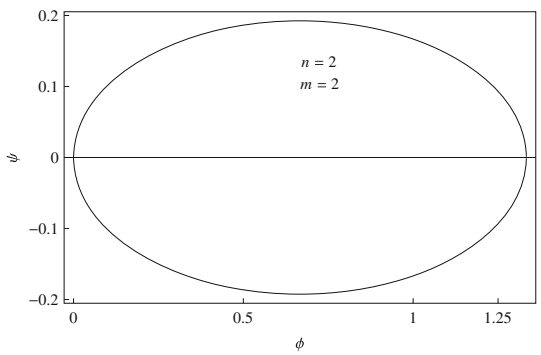

Figure 5. Phase diagram of eq. (19), when $n = 2$, $m = 2$.

present here the plot of the vector field. In future also, we shall not include any plot of such fields, rather we shall assume that these fields converge towards the centre and diverge away from the saddle. We found the solution of (19) in the form

$$u(x,t) = 1.333333\sin^2(0.144338\xi). \tag{21}$$

The trigonometric solution in (21) for $|\xi| \leq 2\pi$ is shown in figure 6. The displayed solitary wave pattern without any exponential tail appears to complement the well-known compacton solution [5] of (4) for $m = 2$ and $n = 2$. Thus, we have an anticompacton solution here.

(b) $m = 3$: For this value of m, the equation similar to that in (19) reads as

$$\phi'' = \frac{v-1}{2v} - \frac{\phi}{6v} - \frac{\phi'^2}{\phi}. \tag{22}$$

Equation (22) has two equilibrium points, $E_1(\sqrt{3(v-1)}, 0)$ and $E_2(-\sqrt{3(v-1)}, 0)$. The equilibrium point E_1 is a centre while E_2 is a saddle. The phase diagram for (22) is shown in figure 7. The phase trajectory consists of two disjoined curves. The centre E_1 lies inside the closed elliptical curve. The saddle E_2 is located on the ϕ-axis at a point in between O and A as shown in the figure. Understandably, the vector field will converge towards E_1 and diverge away from E_2. The solution of (3) for $n = 2$ and $m = 3$ is given by

$$\phi(\xi) = -1.58114\mathrm{cn}^2(-0.18745i\xi, 0.5), \tag{23}$$

where cn(·) stands for the Jacobi elliptic cosine function [16]. The plot of u of (23) as a function of the travelling coordinate ξ is shown in figure 8. The soliton solution presented above has a compact support and is therefore a compacton. Interestingly, we note that the compacton here appears as an internal wave. Moreover, rather than the trigonometric compacton solutions of Rosenau and Hymann [5], the solution in (23) is given in terms of the Jacobi elliptic function.

(c) $m = 4$: The BBM-like equation for $m = 4$ is given by

$$\phi'' = \frac{v-1}{2v} - \frac{\phi}{8v} - \frac{\phi'^2}{\phi}. \tag{24}$$

As in the case of $m = 2$, (24) has only one equilibrium point $E_1((2(v-1))^{1/3}, 0)$ and this is a centre. The phase diagram for (24) is given in figure 9. As expected, the phase trajectory is a closed path and the centre-type equilibrium point lies inside it. The vector field will always be directed towards the centre. We

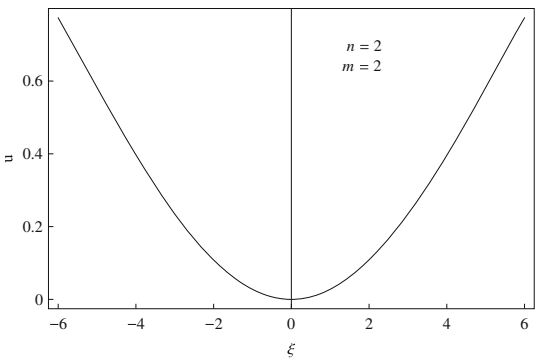

Figure 6. u of (21) as a function of ξ.

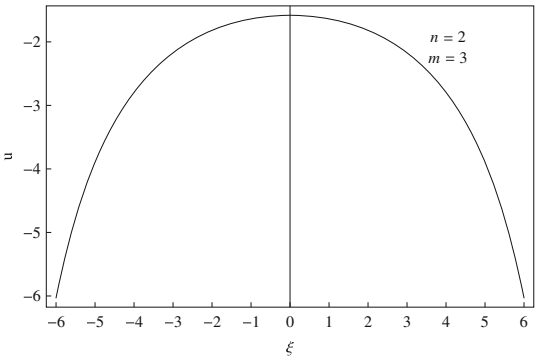

Figure 8. u of (23) as a function of ξ.

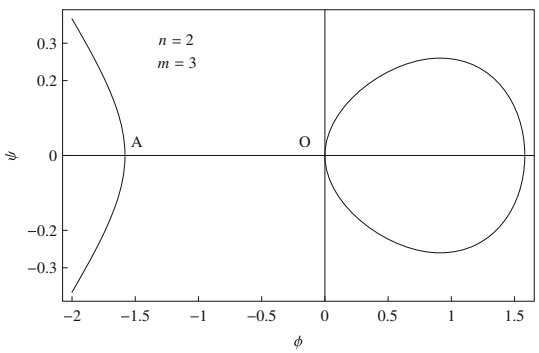

Figure 7. Phase diagram of eq. (22), when $n = 2, m = 3$.

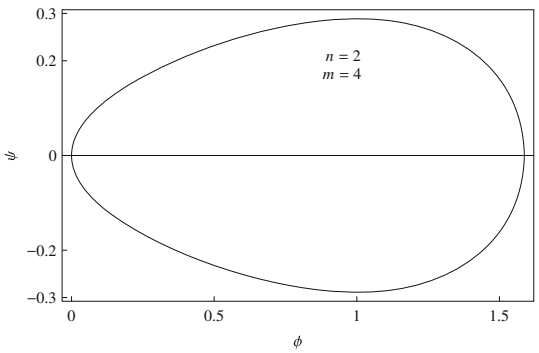

Figure 9. Phase diagram of eq. (24), when $n = 2, m = 4$.

obtained the solution of (24) for $v = 1.5$ in terms of complex valued Jacobi sine and cosine functions. The result is given by

$$\phi(\xi) = \frac{a - b\ \mathrm{sn}^2(y, m')}{c - d\ \mathrm{cn}(y, m')}, \tag{25}$$

where $a = 5.90557$, $b = 2.95279 - 5.11438i$, $c = 3.22185i$, $d = 1.86014$, $m' = 0.5 - 0.866025i$ and $y = 1.130057(1 + i) - (0.045059 - 1.68163i)\xi$. It may appear from the values of a, b, c, d, m' and y that ϕ in (25) represents a complex solution of (24). However, this is not the case. To substantiate our claim we quote below the results of u for three typical values of ξ.

$$u|_{\xi=0} = -7.94848 \times 10^{-17} + 6.89183 \times 10^{-16} i, \tag{26a}$$

$$u|_{\xi=5} = 0.68229 + 2.64838 \times 10^{-8} i \tag{26b}$$

and

$$u|_{\xi=10} = 1.53262 - 1.30542 \times 10^{-8} i. \tag{26c}$$

The result in (26a) shows that both real and imaginary parts of u at $\xi = 0$ are zero while the other two results in (26b) and (26c) indicate that imaginary parts of u for $\xi > 0$ are roughly eight orders of magnitude smaller than the corresponding real parts. We have verified that u is an even function, i.e. $u(\xi) = u(-\xi)$. Thus, as regards (25) the plot of real part of u as a function of ξ will effectively give the variation of u with ξ. In figure 10 we display the plot of u from (25) as a function of ξ. The curve in figure 10 ($m = 4$) closely resembles that in figure 6 ($m = 2$). We have verified that for $n = 2$ all equations with even values of m support anticompacton solutions. In contrast, all such equations for odd values of m support compacton solutions.

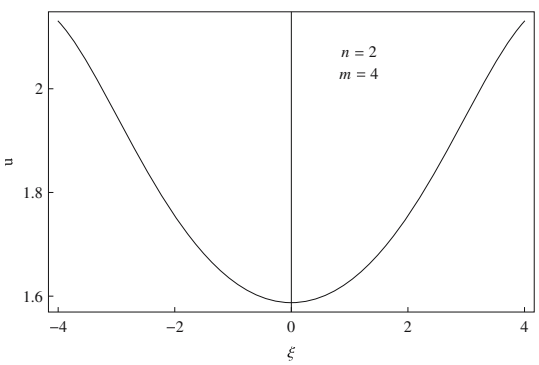

Figure 10. u of (25) as a function of ξ.

3. Dissipative BBM-like systems

Equations of dissipative BBM-like systems for different values of m and n are given in (5). We write this equation in the travelling coordinate and integrate it once to get

$$(1 - v)\phi + a\phi^m + v(\phi^n)'' - \eta\phi' = 0. \tag{27}$$

As before, we have taken the constant of integration as zero. The last term in (27) does not permit one to integrate the equation analytically. As a result, we shall numerically integrate the equivalent first-order equations

$$\psi = \phi' \tag{28a}$$

and

$$\psi' = \frac{(v-1)\phi^{2-n}}{vn} - \frac{a\phi^{m-n+1}}{vn} - \frac{(n-1)\psi^2}{\phi} + \frac{\eta\psi\phi^{1-n}}{vn} \tag{28b}$$

to compute the results for ϕ and ψ as functions of ξ. Admittedly, the parametric plot of ψ vs. ϕ will give the phase diagram of the dissipative system. On the other hand, the plot of ϕ as a function of ξ will display the solution of the equation.

We regard (28a) and (28b) to define a Cauchy boundary value problem such that these equations could be solved by using prescribed values for $\phi(0)$ and $\phi'(0)$. To solve the dissipative equation for a given set of values for m and n we have chosen to work with the value of $\phi(0)$ taken from the corresponding problem for $\eta = 0$ (eq. (3)) as solved earlier by analytical methods. The value of $\phi'(0)$ is always fixed at zero. We solved the initial value problem given in (28a) and (28b) by taking recourse to the use of fourth-order Runge–Kutta method [17] with an appropriate stability check.

3.1 *Dissipative equations with linear dispersive term* ($n = 1$)

As in the non-dissipative case, here we shall present results for $m = 2$, 3 and 4 with a view to visualize how the nonlinearity of the system affects the dissipative wave. In addition, for each equation, we shall present two different sets of results for phase diagram and solution of the equation corresponding to $\eta = 0.1$ and $\eta = 0.5$ with a view to see how the waves in the dissipative medium behave for small and relatively large values for the coefficient of viscosity.

(a) $m = 2$: For $\eta = 0.1$ the phase diagram and the corresponding solution of the system of eqs (28a)

and (28b) are given in figures 11 and 12. Comparing the curve in figure 11 with that in figure 1 we see that due to dissipation the centre-type equilibrium has been converted into an unstable spiral. The phase trajectory appears to diverge from the saddle-type equilibrium point (0, 0) occurred in the corresponding non-dissipative problem. The dissipative effect has changed the soliton solution (15) to an undular bore (figure 12) with a local oscillatory structure behind the bore. These oscillations have their dynamical origin in the periodic solution of the unperturbed system.

In order to see how the formation of the undular bore depends on the viscous effect, in figures 13 and 14 we portray the phase portrait and solution of the dissipative system for $\eta = 0.5$ and compare them with the curves in figures 11 and 12. Closely looking into the curves of figures 11 and 13 we see that for $\eta = 0.5$ the spiraling curve leaves the stable point rather quickly than it did for $\eta = 0.1$. Understandably, the observed change in the phase diagram is likely to have some effect on the dynamics of the bore formation. By comparing the curves in figures 12 and 14 we confirm that this is indeed the case. Here the dissipative force reduces the amplitudes of the periodic waves following the bore and, in fact, the bore is formed due to ripples in the unperturbed system.

(b) $m = 3$: In this case, for $\eta = 0.1$ the phase diagram and solution of the associated BBM-like equation are shown in figures 15 and 16. We now compare the curves in figures 15 and 16 with those in figures 11 and 12 to realize how the nonlinearity of the medium modifies the properties of the dissipative system. The phase trajectories in figures 11 and 15 clearly show

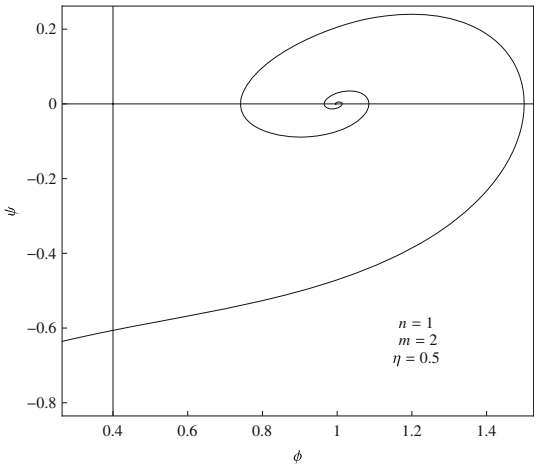

Figure 13. Same as figure 11 but for $\eta = 0.5$.

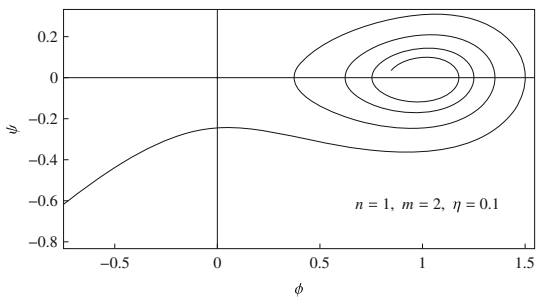

Figure 11. Phase diagram for the dissipative equation with $n = 1$ and $m = 2$ for $\eta = 0.1$.

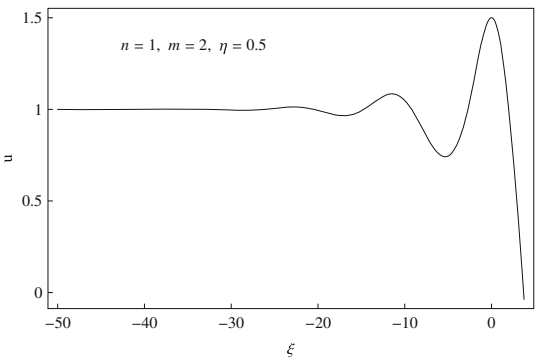

Figure 14. Same as figure 12 but for $\eta = 0.5$.

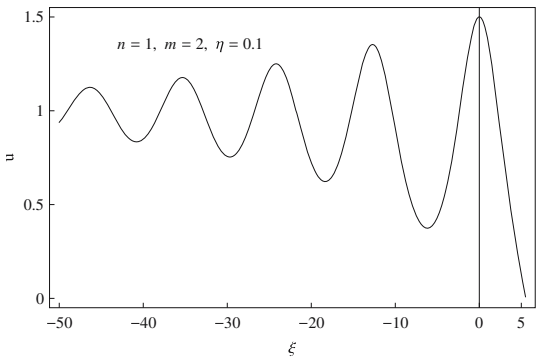

Figure 12. Solution u of the dissipative equation with $n = 1$ and $m = 2$ as a function of ξ.

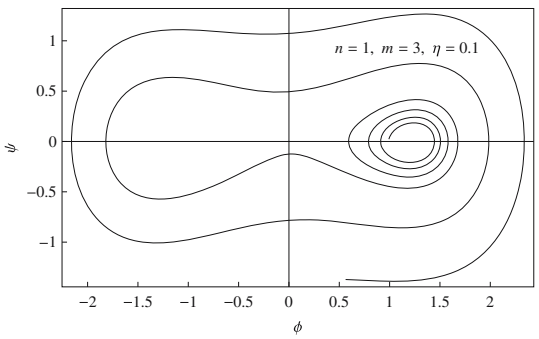

Figure 15. Phase diagram for the dissipative equation with $n = 1$ and $m = 3$ for $\eta = 0.1$.

that as the system becomes more nonlinear, the phase path spirals around one of the centre-type equilibrium points of the system and encircles two other equilibrium points – one centre and the other saddle before it leaves them. The observed change in the phase trajectory appears to have some radical effect on the wave of the unperturbed system. For example, instead of a bore formation at $\xi = 0$ (figure 12), here the wave gains energy from the medium and creates large changes in the medium over very short times (figure 16). These violent changes cause self-steepening of the wave which ultimately resembles a shock front.

For $\eta = 0.5$, the curves corresponding to those in figures 15 and 16 are presented in figures 17 and 18. As is typical for a highly viscous medium, the phase path in figure 17 closely resembles that in figure 13 for $m = 2$. The plot of figure 18 shows that for $m = 3$ the shock-like behaviour of the wave becomes more pronounced.

(c) $m = 4$: The phase diagrams and solutions of the dissipative BBM-like equations for $\eta = 0.1$ and $\eta = 0.5$ are displayed in figures 19–22 respectively. The plots of figures 19–22 closely resemble those in figures 11–14. It thus appears that, as in the case of

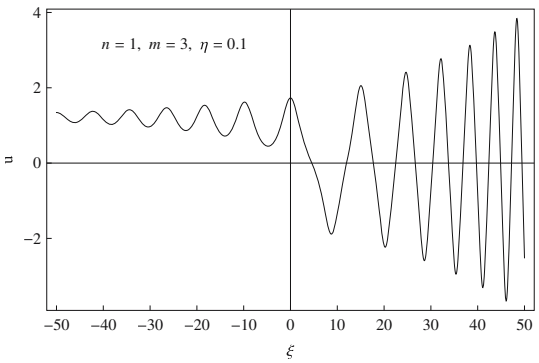

Figure 16. Solution u of the dissipative equation with $n = 1$ and $m = 3$ as a function of ξ.

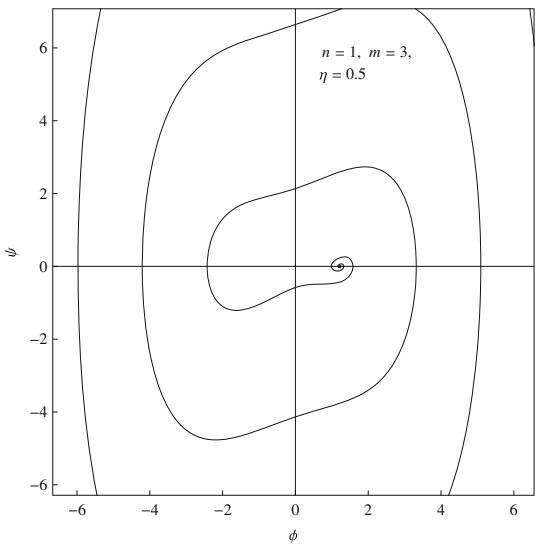

Figure 17. Same as that in figure 15 but for $\eta = 0.5$.

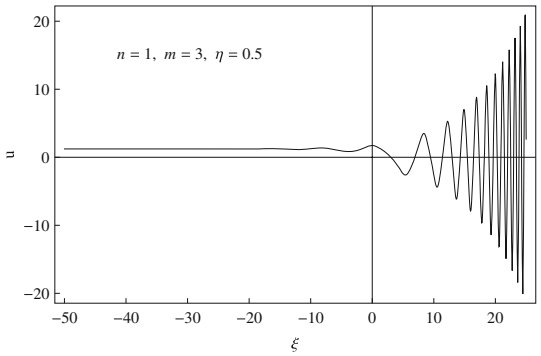

Figure 18. Same as figure 16 but for $\eta = 0.5$.

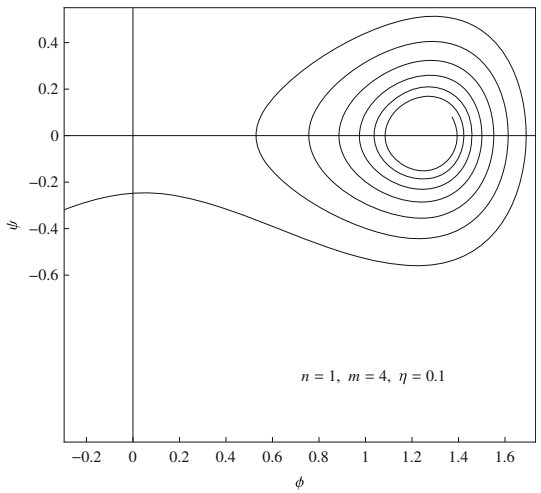

Figure 19. Phase diagram for the dissipative equation with $n = 1$ and $m = 4$ for $\eta = 0.1$.

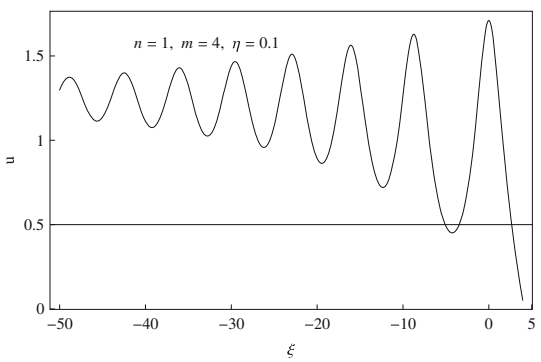

Figure 20. Solution u of the dissipative equation with $n = 1$, $m = 4$ for $\eta = 0.1$ as a function of ξ.

non-dissipative systems, the phase portraits and solutions of the associated BBM-like equation for $m = 2$ are repeated for $m = 4$ even in the presence of dissipation. Similarly, the phase diagram and solution of equations for $m = 5$ are replicas of those for $m = 3$. In general, we found that the dynamics of all even m equations are identical. The same is also true for all odd m equations.

3.2 *Dissipative equations with nonlinear dispersive term* ($n = 2$)

We have seen that non-dissipative generalized BBM equations with nonlinear dispersive terms support soliton-like solutions with compact support. In particular, the solutions of equations with even m are anticompactons and those with odd m are compactons. The anticompacton solutions appear in the form of surface waves while the compacton solutions appear as internal waves. It, therefore, remains interesting to examine the effect of dissipation on these robust objects. We shall achieve this by solving the coupled differential equations (28a) and (28b) for $n = 2$ again by using the algorithms of the fourth-order Runge–Kutta method.

(a) $m = 2$: In this case the phase diagram and plot of u as a function of ξ for $\eta = 0.1$ are shown in figures 23 and 24. In the non-dissipative case, the phase diagram and plot of u as a function of ξ for $n = 2$ and $m = 2$ are presented in figures 5 and 6. The corresponding plots for the dissipative case are displayed in figures 23 and 24. Curves in these figures are drawn by solving the initial value problem using $\phi(0) = 0.01$ and $\phi'(0) = 10^{-6}$. Comparing the curves in figures 5 and 6 with those in figures 23 and 24 we see that due to the effect of dissipation the centre-type equilibrium point has been transformed to a spiral and the anticompacton to an undular bore. As in figure 11 ($n = 1$, $m = 2$ and $\eta = 0.1$), the spiral here also corresponds to an unstable focus. But the phase trajectories in these two cases are somewhat different. We also observe a similar difference between the undular bores of figure 12 ($n = 1$, $m = 2$ and $\eta = 0.1$) and of figure 24. For example, the bore in figure 12 appears at $\xi = 0$ while that in figure 24 appears at $\xi > 0$. Understandably, the observed changes in the phase trajectory and the corresponding solution of the dynamical equation may be attributed to the nonlinearity of the dispersive term.

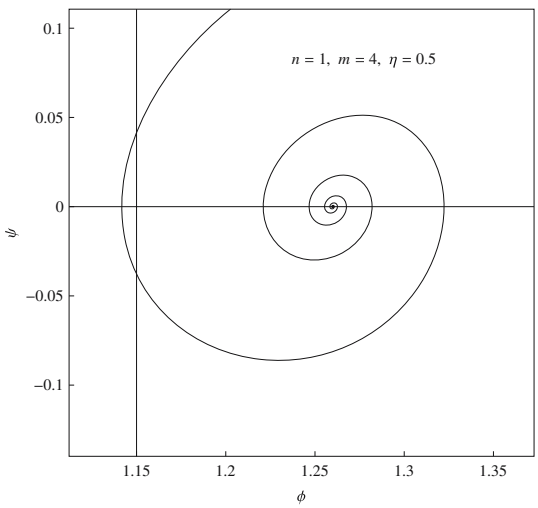

Figure 21. Same as that in figure 19 but for $\eta = 0.5$.

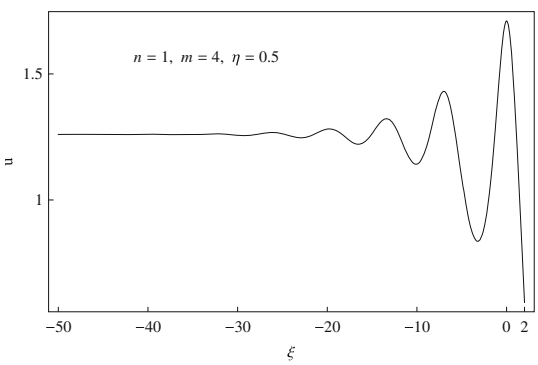

Figure 22. Same as that in figure 20 but for $\eta = 0.5$.

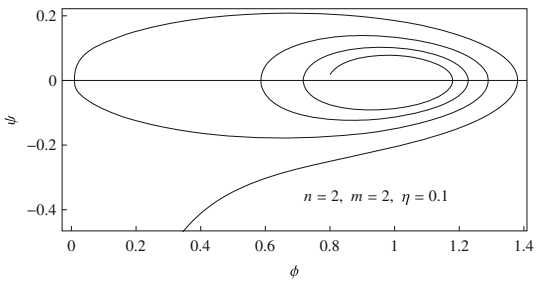

Figure 23. Phase diagram for the dissipative equation with $n = 2$ and $m = 2$ for $\eta = 0.1$.

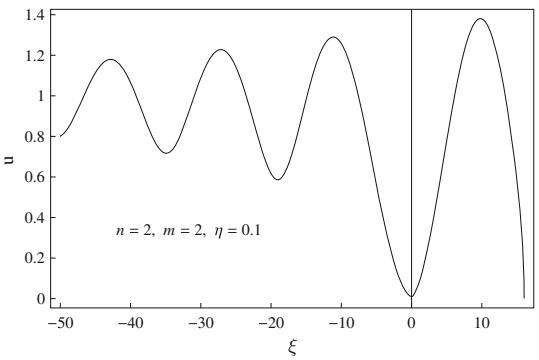

Figure 24. Solution u of the dissipative equation with $n = 2$, $m = 2$ and $\eta = 0.1$ as a function of ξ.

We display in figures 25 and 26 the phase diagram and u as a function of ξ for $\eta = 0.5$. Comparing the curves of these figures with the corresponding curves of figures 23 and 24, we see that the phase trajectory tends to leave the focus more rapidly than it did in figure 23. As with the result in figure 24 the bore in figure 26 is formed at $\xi > 0$. However, the surface oscillation behind the bore appears to be extremely weak. Moreover, the curves in figures 25 and 26 are identical to the corresponding curves for $n = 1, m = 2$ and $\eta = 0.5$ (figures 13 and 14) implying that wave propagation in highly viscous fluid is insensitive to the nonlinearity of the dispersive term in (5).

(b) $m = 3$: Here we solved the coupled differential equations with the initial conditions $\phi(0) = -1.58114$ and $\phi'(0) = 0$ both for $\eta = 0.1$ and $\eta = 0.5$. The appropriate phase portraits and the plot of u as a function of ξ are shown in figures 27–30. The phase diagram in figure 27, when compared with that in figure 7, shows that the dissipative equation is characterized by only one saddle-type equilibrium point. From the plots in figures 8 and 28, we infer that the dissipative effect has converted a compacton into a decaying internal oscillatory wave which tends to disappear for $\xi \gg 0$.

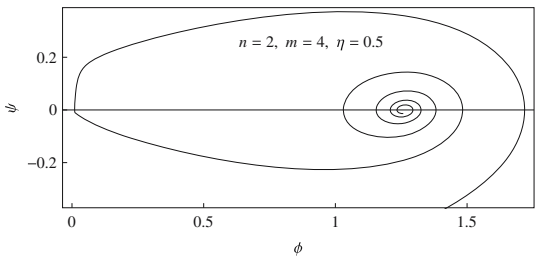

Figure 25. Phase diagram for the dissipative equation with $n = 2$ and $m = 2$ for $\eta = 0.5$.

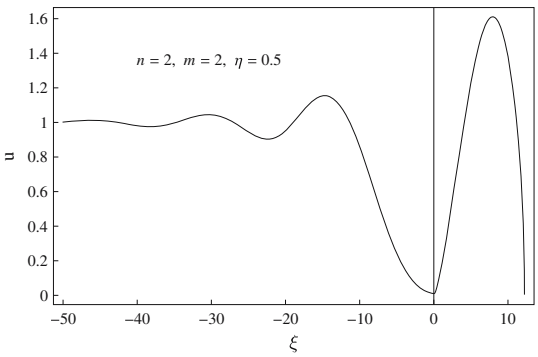

Figure 26. Solution u of the dissipative equation with $n = 2, m = 2$ for $\eta = 0.5$ as a function of ξ.

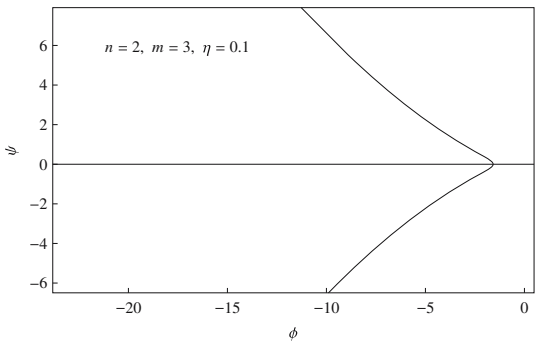

Figure 27. Phase diagram for the dissipative equation with $n = 2$ and $m = 3$ for $\eta = 0.1$.

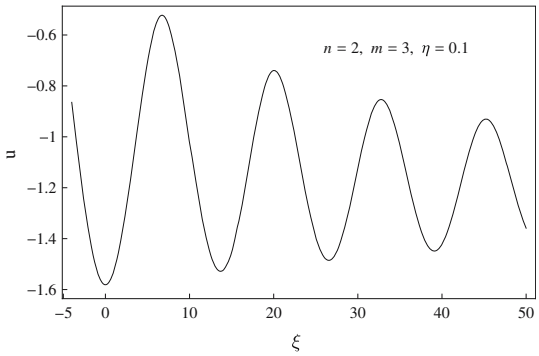

Figure 28. Solution u of the dissipative equation with $n = 2$, $m = 3$ and $\eta = 0.1$ as a function of ξ.

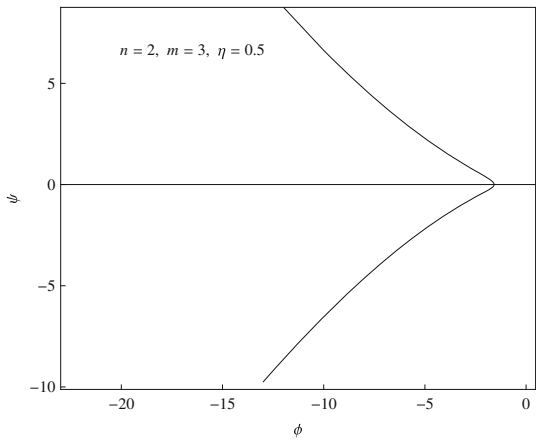

Figure 29. Phase diagram for the dissipative equation with $n = 2$ and $m = 3$ for $\eta = 0.5$.

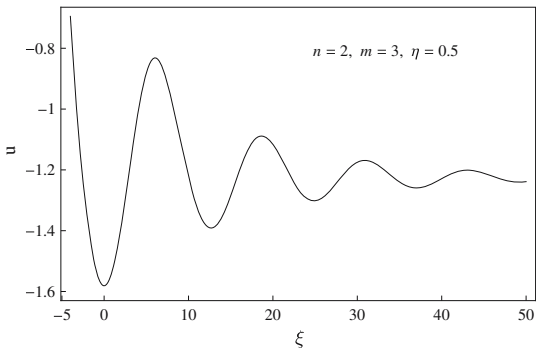

Figure 30. Solution u of the dissipative equation with $n = 2$ and $m = 3$ for $\eta = 0.5$ as a function of ξ.

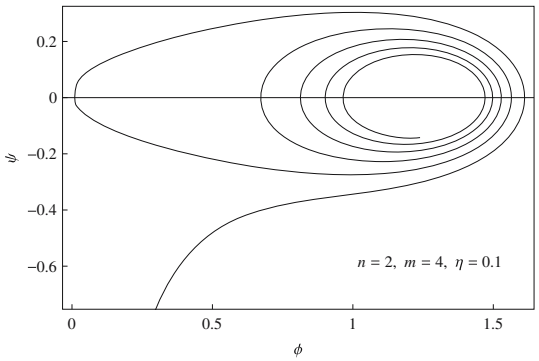

Figure 31. Phase diagram for the dissipative equation with $n = 2$ and $m = 4$ for $\eta = 0.1$.

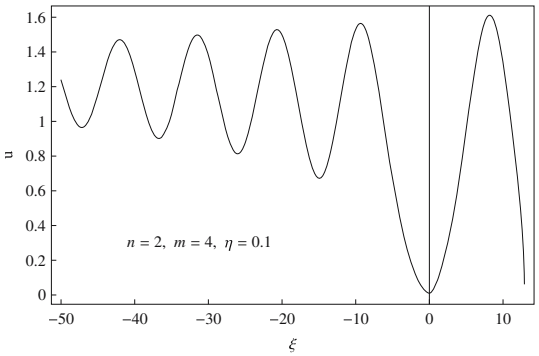

Figure 32. Solution u of the dissipative equation with $n = 2$, $m = 4$ and $\eta = 0.1$ as a function of ξ.

From figure 24 we see that due to the viscous effect the anticompacton appearing in the form of a surface wave absorbs energy from the medium to culminate in an undular bore. On the other hand, the curve in figure 28 shows that the compacton as an internal wave dissipates energy and ultimately takes the form of a decaying oscillatory wave. Plots similar to those in figures 27 and 28 for $\eta = 0.5$ are presented in figures 29 and 30. The phase trajectory in figure 29 is almost identical to that in figure 27. The internal oscillatory wave in figure 30 is also similar to the wave in figure 28 with the only difference that the latter decays very fast.

(c) $m = 4$: It is evidenced by the curves in figures 6 and 10 that in the non-dissipative case the anticompacton solutions for equations with $m = 2$ and $m = 4$ are almost identical. In view of this we solved the coupled dissipative equations for $m = 4$ with the same initial conditions as used for the case study in (a). The appropriate phase diagrams and plots of u as a function of ξ for $\eta = 0.1$ and $\eta = 0.5$ are presented in figures 31–34. The curves in these figures are almost identical to those presented in figures 23–26. We have verified that this is true for all equations with $m = 2k$,

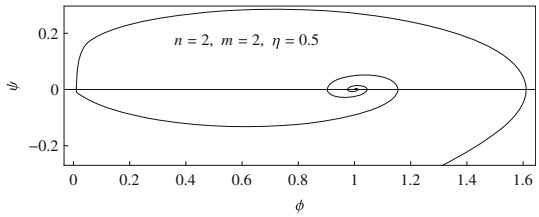

Figure 33. Same as figure 31 but for $\eta = 0.5$.

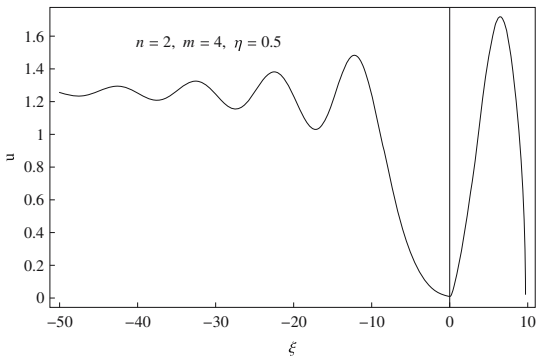

Figure 34. Same as figure 32 but for $\eta = 0.5$.

$k = 1, 2, 3 \ldots$. As with the decaying solutions presented in figures 28 and 30, we note that the results displayed in figures 32 and 34 are also insensitive to the increasing effect of nonlinearity.

4. Conclusion

In addition to the simulation of unidirectional propagation of small-amplitude long waves on the surface of water, the BBM equations (3) and (5) can be used to model a wide variety of physical phenomena that arise in plasma physics, stratified fluid flows, and quantum fluid dynamics. Consequently, there exists a vast amount of literature to study the properties of these RLW equations including their group classification and connection with integrable Riccati and Abel equations [6,18].

In this paper we made use of certain elementary concepts from the dynamical systems theory to examine how the travelling wave solutions of (3) and (5) behave as the nonlinearity and nature of dispersion in the medium modelled by them change. Equation (3) is used to study the propagation of waves in inviscid fluid while (5) refers to a dissipative BBM-like system in a viscous medium.

We constructed the solutions of both non-dissipative and dissipative BBM-like equations in the travelling coordinate ξ. In this coordinate the partial differential equations (3) and (5) reduce to ordinary differential equations with ξ as the independent variable. Thus, by

replacing the pair (x, t) by a single variable ξ we effectively make a transition from field theory to point or classical mechanics. Consequently, the variable may be regarded to play the same role as that of time in Newtonian mechanics.

On a very general ground one knows that in the absence of dissipation Newtonian systems are invariant under time reversal. This means that if $z(t)$ is a solution of the equation of motion, then $z(-t)$ is also a possible solution. The presence of dissipation, however, leads to violation of this discrete symmetry. It is easy to verify that the ordinary differential equations following from (3) for both $n = 1$ and $n = 2$ are invariant under the reversal of ξ. As a result, for every solution presented in §2, we find $\phi(\xi) = \phi(-\xi)$. With regard to parity operation, $\phi \to -\phi$, we observe certain differences between linearly dispersive ($n = 1$) and nonlinearly dispersive ($n = 2$) equations. For instance, equations of even m for $n = 1$ are not invariant under parity operation while the corresponding equations of odd m are found to conserve parity. On the other hand, irrespective of whether m is odd or even, all equations for $n = 2$ are not invariant under the operation $\phi \to -\phi$. These facts appear to have some radical effects on the phase portraits and phase trajectories of the equations.

For $n = 1$ equations of even m have two stable points and phase trajectories are not symmetrical about the ψ-axis. In contrast to this, equations of odd m possess three equilibrium points and phase trajectories exhibit invariance under parity operation. For $n = 2$, each equation of even m is characterized by one centre-type equilibrium point and the phase trajectory lies on the right of the ψ-axis resulting in the violation of reflection symmetry about the ψ-axis. Every odd m equation has two equilibrium points – one centre lying on the right of ψ-axis and the other saddle situated on the left of the line $\psi = 0$. Consequently, as in the case of even m, phase trajectories of odd m equations also violate the reflection symmetry.

Although the equations of even m and odd m for $n = 1$ exhibit anomalous behaviour with respect to their phase-space structure, all of them support soliton solutions. It may be of some interest to see how the conserved quantities of (3) change as m increases. The conservation law for any nonlinear evolution equation in $(1 + 1)$ dimensions can be written as $T_t + T_x = 0$ in which T is called the conserved density and X is called the conserved flux. Admittedly, the quantity $P = \int_{\infty}^{\infty} T \mathrm{d}x$ is a constant of motion. Olver [19] in 1979 showed that the non-integrable BBM equation (eq. (3) for $m = 2$) has only three non-trivial conservation laws with the first, second and third conserved densities given by $T_1 = u$, $T_2 = \frac{1}{2}(u^2 + u_x^2)$, and $T_3 = \frac{1}{3}u^3$ respectively. We have verified that these are also the conserved densities for the general equation (3) for $n = 1$. In view of this we have calculated constants of the motion P_1, P_2 and P_3 corresponding to the conserved densities T_1, T_2 and T_3 for equations having different m values. We found that P_1 decreases continuously as m increases. In contrast, P_2 and P_3 first increase as we go from $m = 2$ to $m = 3$ and then decrease continuously with increasing values of m. In the context of water waves, the conservation laws found by Olver are the equivalents of mass, momentum and energy conservation [20]. Thus, the observed behaviour of P_1, P_2 and P_3 provides us with a demonstration for the effect of nonlinearity on the conservation laws of physical systems modelled by linearly-dispersive BBM-like equations.

The solutions of dissipative BBM-like equations appear to exhibit some physically interesting features. For example, due to dissipative effects, the soliton solutions of (3) for even values of m are transformed into undular bores while those for odd m values resemble the shock waves. With regard to the solutions of nonlinear dispersive equations we note that, as in the case of solitons of even m equations, the anticompactons are transformed to undular bores by the effects of dissipation. On the other hand, due to dissipative effects, the compacton tends to vanish like the solution of an over-damped harmonic oscillator.

The solutions of dissipative BBM-like equations appear to exhibit some physically interesting features. For example, due to dissipative effects, the soliton solutions of (3) for even values of m are transformed into undular bores while those for odd m values resemble the shock waves. With regard to the solutions of nonlinear dispersive equations we note that, as in the case of solitons of even m equations, the anticompactons are transformed to undular bores by the effects of dissipation. On the other hand, due to dissipative effects, the compacton tends to vanish like the solution of an overdamped harmonic oscillator.

The right sides of the first-order differential equations (10a) and (10b) are continuous function of $\phi = (y^{1/n})$. But there can be situations when this is not true. In that case, smooth travelling wave equations support non-smooth travelling wave solutions [21]. Here one needs to consider bifurcation of phase portraits in order to disclose the new features of the non-smooth solutions. Recently, such a problem has been studied by Zhang and Tang [22] who, with particular attention to NoviKov equation, demonstrated the existence of

two peakon or two cuspon solutions for the same wave speed. The dissipation-modified KdV equation can model solitary excitation in a liquid layer [23]. Triki [24] used the so-called sine–cosine method to obtain parametric conditions for the existence and uniqueness of exact solution of such an equation.

Acknowledgement

The authors would like to thank Drs Sk Golam Ali and Amitava Choudhuri for their kind interest in this work.

References

[1] D H Peregrine, *J. Fluid Mech.* **27**, 815 (1967)
[2] T B Benjamin, J L Bona and J J Mahony, *Phil. Trans. R. Soc. London Ser. A* **272**, 47 (1972)
[3] S Yandong, *Chaos, Solitons and Fractals* **25**, 1083 (2005)
[4] L Wang, J Zhou and L Ren, *Int. J. Nonlinear Sci.* **1**, 58 (2006)
[5] P Rosenau and J N Hyman, *Phys. Rev. Lett.* **70**, 564 (1993)
[6] S C Mancas, G Spradlin and H Khanal, *J. Math. Phys.* **54**, 081502 (2013)
[7] G A El, R H J Grimshaw and A M Kamchatnov, *Chaos* **15**, 037102 (2005)
[8] T B Benjamin and M J Lighthill, *Proc. R. Soc. London Ser. A* **224**, 448 (1954)
[9] A V Gurevich and L P Pitaevskii, *Zh. Eksp. Teor. Fiz.* **65**, 590 (1973), *Sov. Phys. JETP* **38**, 291 (1974)
[10] L Zhang and A Chen, *Proc. Rom. Acad. Ser. A* **15**, 11 (2014)
[11] P Razborova, L Moraru and A Biswas, *Rom. J. Phys.* **59**, 658 (2014)
[12] R Abazari, *Rom. Rep. Phys.* **66**, 286 (2014)
[13] A Biswas, *Nonlin. Dynam.* **59**, 423 (2010)
[14] P Sanchez, *Rom. J. Phys.* **60**, 379 (2015)
[15] K T Alligood, T Sauer and J A Yorke, *Chaos*: *An introduction to dynamical systems* (Springer-Verlag, New York, 1997)
[16] E T Whittaker and G Watson, *A course of modern analysis* (Cambridge University Press, Cambridge, 1988)
[17] J B Scarborough, *Numerical mathematical analysis* (Oxford and IBH Pub. Co. Pvt. Ltd., New Delhi, 1993)
[18] P A Clarkson, *J. Phys. A*: *Math. Gen.* **22**, 3281 (1989)
M S Bruzon and M L Gandarias, *Int. J. Math. Models Methods Appl. Sci.* **4**, 527 (2012)
S C Mancas and H C Rosu, *Phys. Lett. A* **337**, 1434 (2013)
[19] P J Olver, *Math. Proc. Camb. Phil. Soc.* **85**, 143 (1979)
[20] S Hamdi, B Morse, B Halphen and W Schiesser, *Nat. Hazards* **57**, 609 (2011)
[21] J W Shen, W Su and W Li, *Chaos, Solitons and Fractals* **27**, 413 (2006)
[22] L Zhang and R Tang, *Proc. Rom. Acad. Ser. A* **16**, 168 (2015)
[23] A N Garazo and M G Velarde, *Phys. Fluids A* **3**, 2295 (1991)
[24] H Triki, *Rom. J. Phys.* **59**, 421 (2014)